Nonclassical dimension-dependent kinetics of a photobleaching reaction in a focused laser beam ''phototrap''

Anna L. Lin,[1,*] Eric Monson,[1,2,†] and Raoul Kopelman[1,2,‡]
[1]*Department of Chemistry, University of Michigan, Ann Arbor, Michigan 48109-1055*
[2]*Applied Physics Program, University of Michigan, Ann Arbor, Michigan, 48109-1120*
(Received 11 March 1997)

A focused laser beam acts as both a ''phototrap,'' bleaching fluorophore molecules that diffuse into the beam path, and as a confocal probe, detecting the excited, unbleached fluorophore molecules still present in the trap. With this focused laser beam, we observe anomalous asymptotic rate laws similar to those predicted for a diffusion-controlled elementary trapping reaction $A+T\rightarrow T$ in both one and two dimensions. One-dimensional diffusion-limited trapping kinetics are observed in capillaries with 10 μm diameters, while two-dimensional (2D) diffusion limited trapping kinetics are observed with unstirred samples having a quasi-2D geometry. However, in the presence of stirring, the 2D samples exhibit the classical, constant trapping rate. [S1063-651X(97)06708-1]

PACS number(s): 82.40.−g, 05.40.+j

I. INTRODUCTION

The kinetic rate laws of diffusion-limited elementary reactions in low dimensions predict an anomalous time dependence in the absence of convection [1–12]. Both perfect and imperfect pseudounary trapping reactions in dimensions $d\leqslant 2$ are expected to exhibit the same asymptotic nonclassical behavior, that results from the creation of a zone around the trap in which the reactant is depleted. This depletion zone grows with a particular time dependence which is proportional to R, the *reaction rate* [9]. This is in contrast to the Smoluchowski kinetic rate law for pseudounary reactions, for which the depletion zone is of constant size over the entire time course of the reaction. Thus, while in well-stirred systems one expects to observe the classical kinetic rate law, in unstirred systems, with diffusion but not convection, one should observe nonclassical reaction kinetics. We give here a straightforward experimental demonstration of such nonclassical behavior for a reaction confined to a capillary tube or to a quasi-two-dimensional geometry. We contrast the nonclassical results found in these samples with the classical result found for the same reaction when in a stirred system.

Classically, for the $A+T\rightarrow T$ trapping reaction, the time *independent*, mean-field rate law $R\sim$ const is assumed to be valid in all dimensions. In three dimensions, the asymptotic rate of diffusion-limited trapping does indeed follow the predicted mean-field rate law [1], as it also does in two dimensions, the critical dimension, except for a logarithmic correction term [8]

$$R\sim\frac{\text{const}}{\ln(t)}. \tag{1}$$

In one-dimensional (1D) geometries, however,

$$R\sim t^{-0.5}, \tag{2}$$

i.e., an asymptotic time dependence is predicted for both perfect [1] and imperfect [2] trapping reactions. Previous experimental investigations of trapping reactions [13] have been carried out in the solid state [14–21] and in a liquid solution phase [17,19]. However, these experiments were performed at low temperatures and thus the reaction kinetics observed for trapping were not well separated from a binary $A+A\rightarrow 0$ reaction process that occurred simultaneously. Also, the effect of stirring on the reaction processes was not or could not be investigated in these experiments.

In this work, we measured the trapping rate of fluorescein free acid in pH 7.6 phosphate buffer solutions contained within 10-μm-i.d. capillary tubes (quasi-1D). For comparison, we also measured the trapping rate of the same solution confined between a cover slip and a microscope slide and in a cylindrical trough. The combined geometry of the sample and the focused laser beam (see Fig. 1) caused the latter two systems to be quasi-2D. The trap in these experiments is the focused laser beam ''phototrap,'' which photobleaches the fluorophores diffusing into it. Here we consider the photobleaching of the fluorophore to be the trapping process since it renders the fluorophore invisible to our detection system and thus ''annihilated.'' Because the fluorophore does not necessarily bleach as soon as it diffuses into the beam path, the phototrap is an imperfect trap and thus a case of general validity. We note that there is an interesting analogy with an enzymatic heterogeneous catalysis [20].

Using Monte Carlo simulations, we verified that the relative number of fluorophores in the trap is directly proportional to the trapping rate, a finding also reported from our laboratory at an earlier time [9]. Experimentally, we demonstrated the nonclassical kinetics for our unstirred low-dimensional reactors, including its dimension-dependent nature.

II. METHODS

A. Experimental setup and procedure

Fused silica capillaries (Polymicro Technologies Inc.) with 10 μm inside diameters and 150 μm outside diameters

*Electronic address: alin@u.chem.lsa.umich.edu
†Electronic address: emonson@umich.edu
‡Electronic address: kopelman@umich.edu

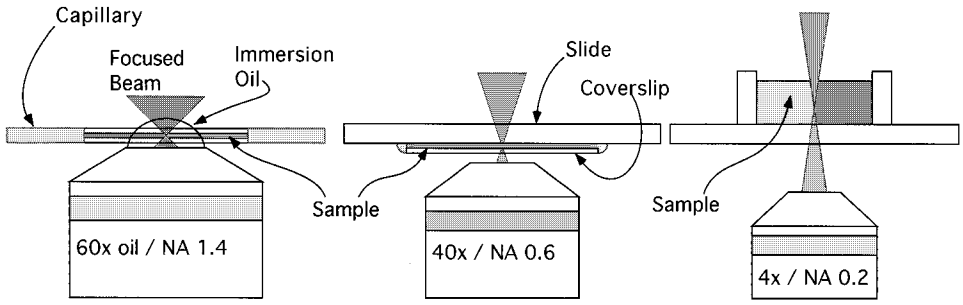

FIG. 1. Schematic of combined sample and focused laser beam ''phototrap.'' These geometries result in quasi-one- and quasi-two-dimensional systems.

were used as quasi-1D reaction vessels. We cut the capillary into pieces with lengths of approximately 10–15 cm and burned an optical window in the fluorescent polyimide outer coating of the capillaries by soaking a central portion of the length of the capillary in 100 °C fuming sulfuric acid for 1 h. The ''reactant'' solutions consisted of a known concentration of the free acid form of fluorescein in *p*H 7.6 phosphate buffer aqueous solution. The buffered *p*H 7.6 solution was necessary for complete dissolution of the fluorescein at a concentration of $1\times10^{-5}M$ and also provides a stable ionic environment for the fluorescein free acid. Fluorescein free acid is in its neutral form at *p*H 7.6, thus we did not have to consider the double layer effect that can occur between ions in solution and the capillary walls. Spectroscopic grade fluorescein free acid was purchased from Aldrich and used without further purification. The phosphate buffer solution was prepared using deionized water and monobasic and dibasic potassium phosphate, both purchased from Aldrich. To fill a 10-μm-i.d. capillary with the aqueous fluorophore solution, we inserted it into the end of a 21 gauge syringe needle and sealed it inside of the needle with glue. A 5-cc syringe was then used to suck the solution into the capillary.

We also confined a drop of the same fluorescein solution between a 22×22 mm^2 Corning No. 1 coverslip and a Gold Seal microscope slide. A clear acrylic shellack was applied to the edges of the coverslip to seal the coverslip to the microscope slide. We measured the thickness of the solution to be approximately 3–8 μm.

The other sample geometry employed was a cylindrical trough with a flat bottom. The diameter of the trough was 2.1 cm and the height was 1.3 cm. The wall of the trough was made of Pyrex glass tubing and the bottom of the trough was a glass microscope slide. For the experiments, the trough was filled approximately two-thirds full with the standard buffered $1\times10^{-5}M$ fluorescein free acid solution. Gelled samples were prepared by adding to the fluorescein solution 0.5 wt.% low-melting-temperature agarose, purchased from Sigma. The purpose of gelling some of the solutions in the trough samples was to determine if there was any convection present that was strong enough to override diffusion as the primary form of mass transport in these experiments. This was accomplished by comparing the trapping rates in gelled versus nongelled samples. Some of the nongelled samples were vigorously stirred by blowing N_2 gas over the top of the solution.

The experimental setup is depicted in Fig. 2. We used lenses to expand and then refocus the beam of an Ion Laser Technology model No. 5490AWC-0 Ar^+ laser, which was then sent to the back port of an Olympus IX70 inverted optical microscope configured for epi-illumination, so as to create a confocal image plane in which the 488-nm Ar^+ laser line was focused to approximately a 2 ± 1 μm diameter and then defocused to approximately a 10 ± 1 μm diameter. The sample sat in the image plane such that the focus of the beam was approximately in the center of the capillary. A high numerical aperture 60× objective, $\mathcal{NA}=1.4$, was used with index of refraction matching oil, $n=1.47$, to minimize aberrations of the beam shape passing through the capillary. The use of this high numerical aperture objective necessitated a capillary outside diameter of less than 200 μm. For the coverslip and trough samples, a 40× and 4× objective, respectively, were used in place of the 60× objective. Fluorescence was detected by an EG&G model No. SPCM-200 avalanche photodiode (APD) that has a 100 μm active area diameter. The APD was connected in series to a photon counter (EG&G, Model No. 1109) and a Tektronix model No. TDS 420 digital ocsilloscope. The signal collected from the APD was processed by the photon counter as a logarithmic value of counts per time bin and then converted to a voltage. This voltage output was grabbed by the digital ocscilloscope with 100 ms per point. The ocsilloscope stored the output over the time course of the experiment. The data were then transferred from the oscilloscope to a 486 PC computer using TEKDIG software, for storage and analysis.

The Ar^+ laser was used at 20 mW power. Thus the beam has a power density that varies from 6.3 to 0.03 mW/μm^2, approximately, as we defocus the beam from 2 ± 1 to 30 μm, for example. The focus of the beam was expanded such that it filled the entire cross-sectional area and traversed the diameter of the capillary, thus rendering the trapping kinetics effectively 1D. For a given capillary diameter, the effect of a small trap with high photobleaching efficiency per

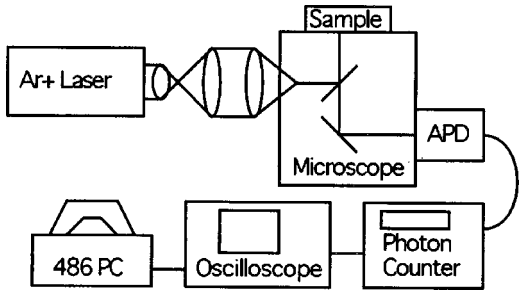

FIG. 2. Schematic of the experimental setup.

unit area, compared to a larger phototrap with lower photobleaching efficiency per unit area, was studied via Monte Carlo simulations (see below).

In the remaining samples, those created by sandwiching sample solution between two glass slides and those created by filling a trough with regular or gelled sample solution, the focused beam is directed through the center of the sample, perpendicular to its largest plane. This geometrical arrangement results in effectively 2D trapping kinetics for those samples. The intensity (proportional to the number of molecules in the trap), measured via confocal fluorescence detection, was monitored as a function of time.

B. Simulation

Monte Carlo methods were used to simulate the diffusion-limited trapping kinetics of the process $A+T\rightarrow T$, where T designates a trap and A designates the diffusive particles that annihilate upon contact with the trap. We landed the A particles randomly on a lattice with no excluded-volume condition. The lattice is a two-dimensional lattice, which has a length that is many orders of magnitude longer than the width (striplike), with reflective boundary conditions in both directions. The trap consists of a designated number of adjacent sites at the end of the lattice. The simulations model the reaction-diffusion process in the usual way [22]. Briefly, particles perform random walks on the lattice by each moving once, randomly, in one of four directions (on 2D lattices) in one time step. If a particle attempts to move onto one of the trapping sites, it is annihilated (removed from the lattice) with a probability p.

In the simulations reported here, the lattice size used was $(6\times10^4)\times25$ sites and initial particle densities were two particles per site. The trap length was one site and the trap width was varied from $W=1$ to $W=25$. For each trap area used, the reaction probability p was chosen such that the total integrated reaction probability of the trap was the same; e.g., for an integrated reaction probability $P_{tot}=1$, we constructed two traps: one consisting of a single lattice site with the local trapping probability p equal to 1 and the other consisting of 25 lattice sites, each with $p=0.04$. We conducted simulations in this manner for three different integrated trapping probabilities.

C. Data analysis

Data were collected linearly in time for both the experiments and the simulations. In the experiments, the photon counts are integrated over 100-msec time bins. In the simulations, the value of the number of particles in the trap is summed over 10-step time bins. Since, for the quasi-1D capillary samples, we are interested in determining the power-law dependence of the trapping rate R as a function of time and we are measuring the instantaneous population of fluorophores at the trap, which is proportional to the rate, we choose to plot the data on a log-log scale. To obtain a properly weighted fit, we wrote a C language code that averaged the linearly collected data over time ranges that increase as powers of 10 and result in ten data points per decade. The data were then fit with a linear least-squares fitting program.

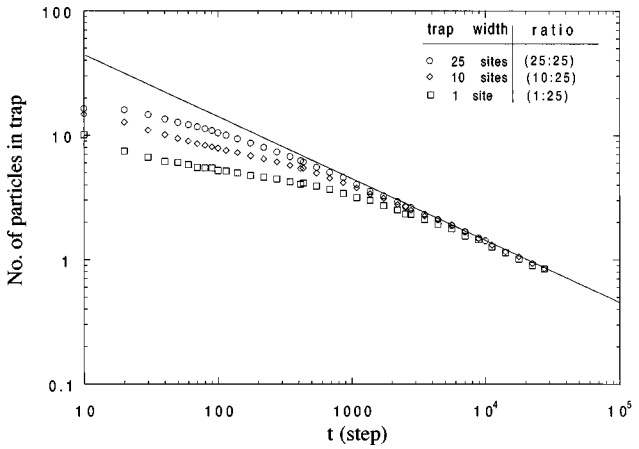

FIG. 3. Simulated density of particles in traps of size [(length)$\times$(width)] 1×25, 1×10, and 1×1 sites vs time. The (trap width)/(lattice width) ratios are 25/25, 10/25, and 1/25 from the top to the bottom curve, respectively. The trapping probability per site in the trap is $p=0.04$, 0.1, and 1 for the top to bottom curves, respectively. The line has a slope of -0.5.

No data were ''thrown out'' using this method. For the quasi-2D experiments, the data were averaged over 50-msec time ranges.

III. RESULTS AND DISCUSSION

A. Monte Carlo simulation: Effect of quasi-1D geometry on trapping rate at early times

Figure 3 is a plot of the number of particles in the trap vs time for Monte Carlo simulations of trapping reactions on $(6\times10^4)\times25$ site lattices. Shown in this figure are data from simulations done on lattices 25 sites wide and with trap sizes [length$\times$width] $=1\times25$, 1×10, and 1×1 sites. The corresponding trapping probabilities per site were $p=$ 0.04, 0.1, and 1, respectively. The data shown are the average of 100 runs collected linearly over 3×10^4 simulation time steps and then further averaged, using the method described in the preceding section, to yield ten data points per decade on a log-log scale.

For a given integrated trapping probability, we studied the effect of the ratio of (trap diameter)/(capillary diameter) on the efficiency of exhibiting one-dimensional trapping behavior. Simulations in which we vary the (trap diameter)/(lattice diameter) ratio, while keeping constant the trapping probability integrated over all trap sites, revealed that a larger trap size with a lower per site trapping efficiency exhibits the anomalous 1D behavior more quickly than a smaller trap with a proportionately larger per site trapping efficiency. Given a certain laser power, this means that we can expect to observe the desired anomalous 1D trapping rate earlier if we use a phototrap that is defocused to fill the cross-sectional area of the capillary, even though it has a lower power density. In contrast, a higher power density phototrap that is more tightly focused and does not fill the cross-sectional area of the capillary will be less efficient in exhibiting 1D behavior of the trapping rate.

The asymptotic behavior of the number of particles in the trap follows a $\sim t^{-0.5}$ power law in time for all three cases, as can be seen by their adherence to a slope of -0.5 on the

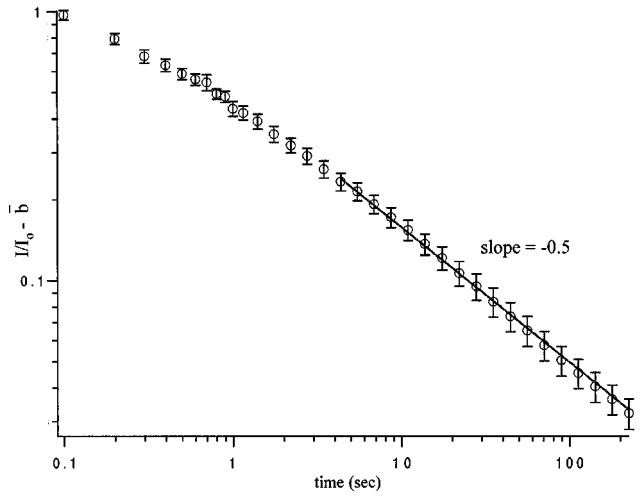

FIG. 4. Intensity vs time data for the 1D phototrapping experiments. Points are experimental data (average of six runs). The solid line has a slope of -0.5.

log-log plot (Fig. 3) at late times. The shallow early time slopes of the curves for the different (trap width)/(lattice width) ratios are due to the imperfect trapping, which results from two different sources: (i) $p<1$ for trap sites, where p is the probability that a particle is trapped if it lands on a site that is designated as part of the trap, and (ii) a (trap width)/(lattice width) <1.

B. 1D phototrapping experiments

Intensity vs time, measured at a 10-μm confocal light trap in a 10-μm-i.d. capillary with the orientation shown in Fig. 1, is plotted in Fig. 4 on a log-log scale. The fluorescence intensity is in arbitrary units and the circles in Fig. 4 are the normalized, averaged values of six independent runs, corrected for the background by subtracting $\overline{b}$, the average, normalized intensity contributed by the background.

The slope of the plot, $I/I_0-\overline{b}$ vs t in Fig. 4 is 0.49 ± 0.07. To obtain $\overline{b}$ the averaged data are fit over different time intervals, ranging from $t=1$ to 225 sec to $t=70$ to 225 sec, by a linear least-squares regression to the form

$$\frac{I(t)}{I_0}=b+at^{-\gamma}, \tag{3}$$

where γ is the best fit slope to the data and a is an arbitrary fitting parameter. The average value obtained for the fitting parameter b was $\overline{b}=0.028$. This value was subtracted from the averaged I/I_0 and the resulting data were fit, over different time intervals, to $y=at^{-\gamma}$, yielding $\gamma=0.49\pm0.07$. The error associated with this slope takes into consideration the upper and lower bounds of the values for b obtained by fitting Eq. (3) over different time intervals.

Note that we were unable to determine experimentally a definite background signal because of the long times required to obtain additional decades of data. A mechanical drift of only a few micrometers in the alignment of the excitation source, sample, and detector can result in a substantial change in the measured fluorescence intensity in the quasi-1D experiments. Our system undergoes such a drift

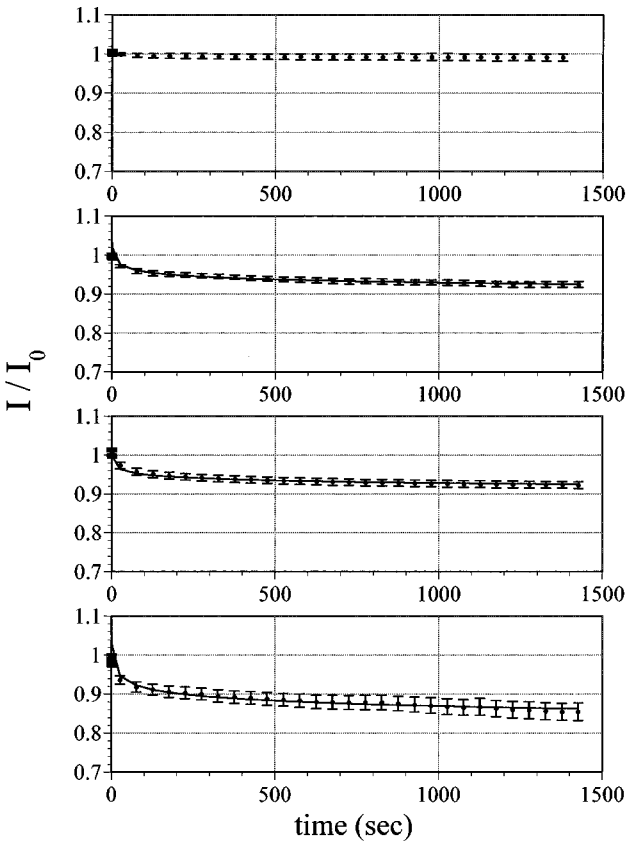

FIG. 5. Intensity vs time data for 2D phototrapping experiments. The normalized, averaged fluorescence intensity obtained from (a) stirred trough samples (7 runs), (b) nongelled trough samples (7 runs), (c) gelled trough samples (11 runs), and (d) coverslip samples (11 runs) are shown. See the text for an explanation of sample types. Points are experimental data. The lines in (b)–(d) are the fits to $y=a/(\log_{10}b+\log_{10}t)$ over the range $t=25$–1400 sec.

over a period of hours, inhibiting us from taking runs that last longer than an hour or two and thus limiting our ability to experimentally determine the inherent combined background intensity of the system and the sample.

The early time data of Fig. 4 exhibit a shallower slope than the longer time data, probably because of the imperfect photobleaching (trapping) of the fluorophore by the focused laser beam trap. The shallower (>-0.5) early time slope, resulting from imperfect trapping, can also be seen in the simulation results plotted in Fig. 3. Since we are able to observe a constant trapping rate in time for the stirred phototrapping reaction [Fig. 5(a)], it seems reasonable to attribute the time-dependent $R\sim t^{-0.49\pm0.07}$ trapping rate of the photobleaching reaction observed in the capillaries to dimension-dependent diffusion-limited trapping kinetics.

B. 2D phototrapping experiments

Figure 5 shows data of intensity vs time obtained under the different 2D trapping geometries described in Sec. II. We test the data for both power-law and logarithmic expressions.

Figure 5(a) is a plot of intensity vs time acquired when the phototrap was directed through a cylindrical, flat bottomed trough filled with stock fluorescein solution. The solutions were *stirred* (see Sec. II A) over the entire time scale

of the experiment. The data points, representing the average of seven independent runs in which the normalized fluorescence intensity at the trap is recorded as a function of time, are plotted on a linear scale. The slope of the linear least-squares regression of the averaged data, fit with a power law, gives the time dependence of the intensity: $I/I_0 \sim t^{-0.0020\pm0.0005}$, i.e., a power of -0.002. In all of the quasi-2D experiments, the background did not contribute significantly to the fluorescence since a much larger sample volume is illuminated. This also makes the quasi-2D experiments less sensitive to mechanical drift. Figure 5(b) is also a plot of intensity vs time for data acquired at the phototrap when it was directed through the trough. However, here the trough was filled with a fluorophore solution that was *not* stirred. The data points are the average of seven runs and the least-squares fit with a power law yields, from the slope, a time dependence of $I/I_0 \sim t^{-0.09\pm0.02}$. The solid lines in Figs. 5(b)–5(d) are the function $I/I_0 = a/\ln(bt)$, where a and b are fitting parameters and the function is fit to the data over the range of $t = 25-1400$ sec.

Figure 5(c) is a plot of intensity vs time of data acquired at the phototrap when it was directed through samples indentical to those used to obtain the data shown in Fig. 5(b), *except* that the solution was gelled to ensure the absence of convection. The data points are the average of 11 runs and the least-squares regression of this data fit with a power law gives $I/I_0 \sim t^{-0.13\pm0.02}$. Figure 5(d) is a plot of intensity vs time of data that was acquired when the confocal phototrap was directed through a thin layer of fluorophore solution sandwiched between a coverslip and a microscope slide. The data points are the average of 11 runs and the least-squares regression of these data fit a power law with a slope of -0.11 ± 0.02.

From our simulations, as well as from the results reported by others [9], we know that the density of molecules in an imperfect trap is directly proportional to the flux of molecules to that trap, which in turn is directly proportional to the trapping rate (the rate at which molecules are consumed by the trap). The trapping *rate* [1,2,8–10] is one of the quantitative measures by which the behavior of diffusion-limited trapping is compared to the classical trapping behavior. In our experiments, $I(t)/I_0$ is a measure of the instantaneous relative density of molecules in the trap, which is directly proportional to the instantaneous trapping rate R. Because the geometry of the phototrap is conical and it traverses the short dimension of our samples, perpendicular to the largest plane of the coverslip and trough samples, both of these samples are effectively 2D with respect to trapping kinetics. In Figs. 5(b)–5(d) the fluorescence intensity shows a weak dependence on time, asymptotically, as can be seen by the fit to the logarithmic corrected time curves (solid line) at late times. The weak *effective* power-law dependence is consistent with a logarithmic correction to a constant time dependence of the trapping rate [see Eq. (1)], which is the functional form of the 2D trapping rate law predicted theoretically [1].

Significantly, the stirred system exhibits the classical, time-independent rate law, within the experimental error, predicted for a trapping reaction with a random reactant distribution. (This is also predicted to occur under reaction-limited conditions or in a 3D trapping geometry.) On the other hand, the unstirred systems show definite deviations, which seem to represent the nonclassical case, within the error bounds of the experiment.

IV. SUMMARY

The successful observation of the anomalous, diffusion-limited rate law predicted for a trapping reaction occurring in $(d \leqslant 2)$-dimensional geometries is reported. The trap in these experiments was stationary over the entire duration of the experiment and the transport mechanism of the fluorophores to the trap was either diffusion or intentional stirring. The Monte Carlo computer simulations show that a larger trap coupled with a lower per-site trapping probability results in 1D trapping kinetics faster than a smaller trap with a higher per-site trapping probability if the total integrated trapping probability is the same. The mean-field rate law is not strictly valid in two-dimensions because of the logarithmic correction term, but is completely valid in the presence of convection or other stirring forces. We indeed do observe this trend in our experimental data, where a weak power law (or, alternatively, a logarithmic) dependence of the trapping rate on time is displayed in the 2D unstirred samples, but no time dependence is displayed in the stirred 2D samples, within the experimental error. For the phototrapping experiments done in capillary tubes, a $t^{-0.49\pm0.07}$ time-dependent rate is observed. This agrees well with the anomalous $t^{-0.5}$ dependence predicted for diffusion-limited trapping reactions in a truly one-dimensional space [1,2]. Moreover, the data exhibit the predicted trend: The lower the dimension, the smaller the scaling exponent.

ACKNOWLEDGMENTS

We acknowledge the support provided by NSF Grant No. DMR-9410709.

[1] G. Weiss, R. Kopelman, and S. Havlin, Phys. Rev. A **39**, 466 (1989).
[2] H. Taitelbaum, R. Kopelman, G. Weiss, and S. Havlin, Phys. Rev. A **41**, 3116 (1990).
[3] A. A. Ovchinnikov and Y. G. Zeldovich, Chem. Phys. **28**, 215 (1978).
[4] P. G. de Gennes, C. R. Acad. Sci. Paris **296**, 881 (1983).
[5] K. Kang and S. Redner, Phys. Rev. Lett. **52**, 55 (1984).
[6] P. Argyrakis and R. Kopelman, J. Theor. Biol. **73**, 205 (1978).
[7] R. Kopelman, Science **41**, 1620 (1988).
[8] S. Havlin, H. Larralde, R. Kopelman, and G. H. Weiss, Physica A **169**, 337 (1990).
[9] R. Schoonover, Ph.D. thesis, University of Michigan, Ann Arbor, 1993 (unpublished).
[10] R. Schoonover and R. Kopelman, in *Dynamics in Small Confining Systems*, edited by J. M. Drake, J. Klafter, R. Kopelman, and D. D. Awshalom, MRS Symposia Proceedings No. 290, (Materials Research Society, Pittsburgh, 1993), pp. 255–260.

[11] P. Meakin and H. E. Stanley, J. Phys. A **17**, L173 (1984).
[12] S. Havlin and D. Ben-Avraham, Adv. Phys. **36**, 695 (1987).
[13] R. Kopelman, J. Prasad, and S. J. Parus, in *Molecular Dynamics in Restricted Geometries*, edited by J. Klafter and J. M. Drake (Wiley, New York, 1989), Chap. 6.
[14] C. S. Li, Ph.D. thesis, University of Michigan, Ann Arbor, 1988 (unpublished).
[15] R. Kopelman, C. S. Li, and Z.-Y. Shi, J. Lumin. **45**, 40 (1990).
[16] R. Kopelman, Z.-Y. Shi, and C. S. Li, J. Lumin. **48&49**, 143 (1991).
[17] R. Kopelman, S. J. Parus, and J. Prasad, Chem. Phys. **128**, 209 (1988).
[18] R. Kopelman, Z. Y. Shi, and C. S. Li, J. Lumin. **48&49**, 143 (1991).
[19] R. Kopelman and A. L. Lin, in *Non-equilibrium Statistical Mechanics in One Dimension*, edited by V. Privman (Cambridge University Press, Cambridge, 1997), Chap. 21.
[20] A. L. Lin, M. S. Feldman, and R. Kopelman (unpublished).
[21] J. Prasad and R. Kopelman, J. Phys. Chem. **91**, 265 (1987).
[22] P. Argyrakis, Comput. Phys. **6**, 525 (1992).